Manuscript submitted to:
Cement

A Small-scale Thermogravimetric Method to Measure the Chemical Reactivity of Supplementary Cementitious Materials

Sarah L. Williams[1,2], *Danielle N. Beatty*[1], *Wil V. Srubar III*[1,2*]

[1]Materials Science and Engineering Program, University of Colorado Boulder, 4001 Discovery Dr, UCB 027, Boulder, Colorado, 80303, sarah.l.williams@colorado.edu,

[2]Department of Civil, Environmental, and Architectural Engineering, University of Colorado Boulder, 1111 Engineering Dr, ECOT 441 UCB 428, Boulder, Colorado, 80309

*Corresponding Author: wsrubar@colorado.edu

Abstract:

Partial replacement of ordinary portland cement (OPC) with supplementary cementitious materials (SCMs) is a ubiquitous and effective approach to design concrete mixtures with lower embodied carbon and improved durability compared to plain OPC concrete mixtures. However, the global supply of common industrial SCMs, like fly ash (a byproduct of coal combustion) and blast-furnace slag (a byproduct of steelmaking), is dwindling due to global decarbonization efforts and sustained demand from the concrete industry. The newly standardized ASTM C1897 rapid, relevant, and reliable (R3) test is an effective screening method to measure the chemical reactivity of potential SCMs. However, the sample quantity requirements impede the rapid-throughput screening of new SCM sources that may currently be available only in small quantities. The objective of the current study was to design and validate a small-scale modified R3 test to enable standardized characterization and rapid-throughput screening of novel SCMs. The results substantiate that the ASTM C1897 R3 bound water method can be performed with sufficient accuracy at a much smaller scale (*i.e.*, 0.01 g of SCM per test) using the thermogravimetric method developed and validated herein.

Keywords: Supplementary cementitious materials, chemical reactivity, thermogravimetric analysis, isothermal calorimetry, ASTM C1897, R3 test

1. INTRODUCTION

Concrete, which is comprised primarily of ordinary portland cement (OPC), mineral aggregates, and water, is the most utilized anthropogenic material on Earth. More than 4 billion tonnes of OPC, the key binding material in concrete, are produced annually[1], accounting for approximately 7% of global carbon dioxide (CO_2) emissions[2]. Clinker substitution, a strategy in which OPC clinker is partially replaced by supplementary cementitious materials (SCMs), is the most promising strategy to reduce CO_2 emissions from OPC production in the near term[3,4]. SCMs are chemically compatible with OPC and contribute to the hardened-state properties of concrete through hydraulic and/or pozzolanic activity. Partial replacement of OPC with SCMs of industrial origin (*e.g.*, fly ash, ground granulated blast furnace slag, silica fume) and natural origin (*e.g.*, calcined clays, zeolites, pumice, limestone) is practiced widely around the world.

The use of SCMs reduces environmental impacts of concrete due to the reduction of clinker content while improving the durability of concrete due to densification of the paste microstructure[5]. However, maintaining consistent supplies of many industrial SCMs has recently become challenging[6]. Fly ash, a byproduct from coal combustion, has been the most used SCM in recent decades. While fly ash was once considered an abundant waste material[7], the global supply is now dwindling due to global decarbonization efforts (*i.e.*, switching away from coal power) as well as sustained demand from the concrete industry. For example, coal consumption in the United States declined by almost half over the twelve-year period from 2007 to 2019, falling from 1,045,140 million to 539,420 million US tons[8]. Ground granulated blast furnace slag (hereafter referred to as "slag") is a byproduct of the smelting of pig iron that exhibits latent hydraulic activity as an SCM in concrete. Like fly ash, the supply of slag is also threatened as very high quantities of suitable blast furnace slag are already in use in concrete[3].

Considering this marked decline in supplies of today's most widely utilized SCMs, there is a need for more rapid and versatile standardized protocols for testing the chemical reactivity of potential new sources of SCMs. An ideal reactivity test to screen and qualify SCMs for use in concrete should be quick, accurate, and reproducible while requiring a small sample quantity so that novel sources of potential SCMs can be screened more efficiently. Today, traditional standardized test methods fall short of one or more of these criteria [9].

The strength activity index (SAI) test (ASTM C311)[10], in which OPC is partially replaced by a potential SCM in standard mortars and evaluated by a measure of 28-day compressive

strength, is one of the most utilized conventional methods. Significant drawbacks associated with the SAI method include a relatively long testing time (28 days), prevalence of false positive results (*i.e.*, inert materials passing as reactive)[11,12], high variability due, in part, to the variability of OPC, and high material quantity requirements (>100 g of SCM). The Frattini pozzolanicity test (EN 196-5) can be performed more quickly (8-15 days) and with less material (~4 g of SCM per test)[13]. However, issues regarding accuracy and reproducibility have been noted in the literature that are due, in large part, to the sensitivity of the experimental set-up[9]. Similarly, the Chapelle test[14,15] and the modified Chapelle test (NF P18-513) can be performed in 1 day and only require ~1 g of SCM per test, but these methods have shown poor correlation to 28 day relative compressive strength ($R^2 < 0.50$) as well as poor interlaboratory reproducibility due to the complexity of the experiments[9].

Recently, a rapid, relevant, and reliable (R3) test has been developed to determine the chemical reactivity of potential SCMs in a simplified system[16]. This work and subsequent related work[9,17] were used to develop a new standard, namely ASTM C1897-20: Standard Test Methods for Measuring the Reactivity of Supplementary Cementitious Materials by Isothermal Calorimetry and Bound Water Measurements. ASTM C1897 includes two alternative test methods (Method A and Method B) to assess the chemical reactivity of an SCM in a hydrated paste composed of the SCM, calcium hydroxide, calcium carbonate, potassium sulfate, and potassium hydroxide cured at 40 °C for 7 days. Method A measures heat evolution using isothermal calorimetry while Method B measures chemically bound water using a furnace. No requirement or preference to use Method A or Method B for a given application exists, as both cumulative heat evolution and bound water content have shown good correlation to 28 day relative compressive strength ($R^2 > 0.85$) and excellent interlaboratory reproducibility[9].

A modified R3 test, also sometimes referred to as the pozzolanic reactivity test (PRT), has also been developed by making some key modifications to the R3 system[18,19]. Most notably, potassium sulfate and calcium carbonate are omitted from the system. Research has shown that the addition of sulfates in the R3 test can lead to preferential reaction with aluminous phases to form monosulfo-aluminates and ettringite[19]. Another key difference is that the modified R3 test is carried out for a duration of 10 days at a temperature of 50°C. Particularly for slowly reacting materials, the acceleration provided by the longer duration and higher temperature in the modified R3 test might be more reflective of later-age properties. The modified R3 test also directly

measures calcium hydroxide (CH) consumption which can enable greater distinction between latent hydraulic and pozzolanic reactivity and prediction of calcium oxychloride damage[18].

The objective of this methodological study was to adapt the R3 test as described in ASTM C1897 to use an even smaller sample size (on the order of milligrams) using thermogravimetric analysis (TGA). The original R3 test was chosen for adaptation because, to the authors knowledge, it is the only test that has been optimized and validated via interlaboratory ruggedness and round robin testing[18]. ASTM C1897 specifies that both Methods A and B are to be performed using a sample size of 15 g freshly mixed paste (~2 g of SCM per test). This sample quantity requirement is generally acceptable for screening materials from existing supply chains (*e.g.*, waste materials, industrial byproducts) or geological deposits (*e.g.*, clays, natural pozzolans). However, the sample quantity requirements impede the rapid-throughput screening of novel SCM sources that might currently only be available in small quantities, particularly manufactured, biomanufactured, and/or synthetic materials that do not yet have a consistent supply chain. A small-scale R3 method could also enable efficient, rapid-throughput assessment of different physical and chemical treatments methods designed to improve the reactivity of alternative SCMs. Combined with machine learning and artificial intelligence, the data could lead to the discovery of new physical and chemical treatment methods that improve alternative SCM reactivity.

First, both ASTM C1897 Methods A and B were performed on full-scale (*i.e.*, 15 g) paste specimens containing five different mineral powders spanning a wide range of SCM types. Next, paste samples were prepared across different orders of magnitude by mass including full-scale (15 g), mid-scale (0.15 g), and small-scale (0.015 g) for bound water testing using TGA. It was determined that bound water content was statistically similar regardless of scale or measurement technique, which validated the small-scale modified R3 test proposed herein.

2. MATERIALS AND METHODS

2.1. Materials

Deionized water (DI-H_2O) was used for all experiments. Potassium sulfate (K_2SO_4) and potassium hydroxide (KOH) were obtained from Fisher Scientific (Hampton, NH, USA). A potassium solution was prepared by dissolving 4 g/L (71 mM) KOH and 20 g/L (115 mM) K_2SO_4 in DI-H_2O. The potassium solution was allowed to equilibrate at ambient temperature for at least 1 hour prior to experimentation. Reagent-grade calcium hydroxide, or portlandite, was obtained from Sigma-

Aldrich (St. Louis, MO, USA). Reagent-grade calcium carbonate, or limestone, was obtained from Research Products International (Mt Prospect, IL, USA).

Five mineral powders representing a wide variety of SCM types and reaction mechanisms were obtained for chemical reactivity measurements, as shown in **Table 1**. Common pozzolanic SCM types including calcined clays, natural pozzolans, and industrial pozzolans were represented by metakaolin (MK), diatomaceous earth (DE), and fly ash (FA), respectively. Latent hydraulic materials were represented by ground granulated blast furnace slag (SL). Finely ground quartz (Q) was also included as an inert material to serve as a negative control for chemical reactivity[9,20,21].

Table 1: Summary of mineral powders tested as SCMs used in this study.

Abbreviation	**Material**	**Mechanism**	**Source**	
MK	Metakaolin	Pozzolanic	BASF	Sandersville, GA, USA
SL	Granulated blast furnace slag (Grade 120)	Latent hydraulic	US Concrete	San Jose, CA, USA
DE	Diatomaceous earth	Pozzolanic	PF Harris	Cartersville, GA, USA
FA	Fly ash (Type F)	Pozzolanic	US Concrete	San Jose, CA, USA
Q	Quartz	Inert	Sigma-Aldrich	St. Louis, MO, USA

2.2. Scanning Electron Microscopy/ Energy-dispersive X-ray Spectroscopy (SEM/ EDS)

The microstructure and elemental composition of each unreacted SCM were investigated using a Hitachi SU3500 SEM (Santa Clara, CA, USA) equipped with an Ultim Max EDS detector (Oxford Instruments, UK). A thin layer of powdered sample was mounted on carbon tape and sputter coated with 8-10 nm of platinum. SEM was conducted at a magnification of 1,500x using an accelerating voltage of 10 kV and a working distance of 8-10 mm. Average EDS spectra (*i.e.*, over the entire scan frame) were collected at five randomly selected sites for each sample; the five EDS spectra for each sample were processed in AZtec software and averaged to minimize potential variability due to material heterogeneity.

2.3. Inductively Coupled Plasma Optical Emission Spectrometry (ICP-OES)

A commercial laboratory (Hazen Research, Inc., Golden, CO, USA) was employed to perform quantitative chemical characterization of the unreacted SCMs. ICP-OES was performed using a Perkin Elmer Optima 7300 DV. Prior to analysis, ~0.2 g of each sample were added to a 95%/5% Pt/Au crucible and mixed thoroughly with 2 g fluxing agent (1:1 lithium metaborate/ lithium tetraborate) and 5-10 drops of 25% lithium bromide. Acid digestion was performed using ~90 mL of DI-H_2O, 10 mL of concentrated hydrochloric acid (HCl), and 1 mL of concentrated hydrofluoric acid (HF) in a Teflon beaker, followed by fusion using a Claisse fusion instrument.

2.4. X-Ray Diffraction (XRD)

A Bruker D8 Advance X-ray Diffractometer (Billerica, MA, USA) with Cu Kα radiation (wavelength 1.5406 Å) was used to collect qualitative XRD data for each unreacted SCM powder and selected reacted paste mixtures. Approximately 20 mg of each sample was mixed with isopropyl alcohol and poured onto a silica zero background plate. The isopropyl alcohol was then allowed to evaporate prior to testing. Data was collected from 5-65° 2θ with a step size of 0.02° and a dwell time of 2 sec per step. The current was 40 mA and the voltage was 40 kV. Crystalline phases were identified using Bruker DIFFRAC.EVA software and the International Center for Diffraction Data (ICDD) PDF-4 AXIOM 2019 database.

2.5. Preparation of Paste Samples

Mixtures were proportioned according to ASTM C1897[22]. The SCM-to-portlandite, SCM-to-limestone, and potassium solution-to-solids ratios (by mass) were held constant at 1:3, 2:1, and 6:5, respectively, in accordance with ASTM C1897. For each of the five SCMs in the current study, paste samples were prepared across different orders of magnitude by mass as displayed in **Table 2**. While the mixture proportions stipulated by ASTM C1897 were kept constant for each mix, additional DI-H_2O was added to the 10^{-2} and 10^{-3} mixes to ensure homogeneity and reduce the risk of carbonation due to the smaller sample size. At the largest scale (full-scale), pastes were prepared by combining all the ingredients in a glass beaker and mixing by hand with a metal spatula for 2 min. The other mixes (mid-scale and small-scale) were prepared in microcentrifuge tubes and mixed by pulse vortex for 2 min.

Table 2: Mix designs at multiple scales.

Scale	SCM (mg)	Portlandite (mg)	Limestone (mg)	Potassium Solution (mg)	DI-H_2O (mg)
Full (10^0)	10,000	30,000	5,000	54,000	-
Mid (10^{-2})	100	300	50	540	540
Small (10^{-3})	10	30	5	54	54

2.6. Isothermal Calorimetry (ASTM C1897 Method A)

A TAM Air 8-channel isothermal calorimeter (TA Instruments, New Castle, DE, USA) was used to measure the cumulative heat release of the full-scale paste samples according to ASTM C1897 Method A[22]. The bath temperature was set to 40 °C, and the calorimeter was allowed to equilibrate at 40 °C for at least 24 hours prior to testing. 15 g aliquots of freshly mixed paste were transferred to glass ampoules. The ampoules were hermetically sealed and then loaded into the calorimeter as quickly as possible, which was typically within 2 minutes of the end of mixing. The signal was allowed to stabilize for 75 minutes, and then heat flow data were collected for at least 7 days. Cumulative heat release normalized by mass of SCM was calculated at 3 days and 7 days. Each sample was tested in duplicate.

2.7. Bound Water Content (ASTM C1897 Method B)

Chemically bound water content was determined for the full-scale paste samples according to ASTM C1897 Method B[22] using a furnace. First, 15 g aliquots of freshly mixed paste were transferred to plastic containers, sealed, and then cured in an oven at 40 °C for 7 days. Following curing, the pastes were removed from their containers and crushed to a particle size finer than 2 mm. Each crushed paste specimen was then spread evenly in a thin layer (< 10 mm) in a glass petri dish and returned to the oven to dry at 40 °C for 24 hours. Approximately 5 g of each dried crushed paste specimen were transferred to a ceramic crucible and the mass was recorded. The crucibles were then transferred to a furnace at 350 °C for 2 hours at which time they were removed and allowed to cool for approximately 1 hour. The final mass was recorded. Bound water content was determined by calculating the difference between the mass of the sample before and after heating at 350 °C. Each sample was tested in triplicate.

2.8. Thermogravimetric Analysis (TGA)

TGA was performed on all reacted paste samples (full-scale, mid-scale, and small-scale) using a TA Discovery 5500 (TA Instruments, New Castle, DE, USA) in an inert nitrogen atmosphere. Approximately 10 mg of reacted paste were placed in a platinum pan and allowed to equilibrate at 40 °C. Then, the temperature was ramped up to 350 °C at a rate of 10 °C/min. Bound water content was determined by calculating the difference between the initial mass of the sample at 40 °C and the final mass after heating to 350 °C. Each sample was tested in triplicate.

2.9. Statistical Analysis

Mann-Whitney U tests[23] were performed to examine (1) the influence of measurement technique (furnace vs. TGA) on bound water content for full-scale mixes, and (2) the influence of sample scale by mass (*i.e.*, full-, mid-, small-scale) on bound water content as determined by TGA. The Mann-Whitney U Test was chosen because it is nonparametric and, therefore, does not require any assumptions about the distribution of the data.

3. RESULTS AND DISCUSSION

3.1. Characterization of Unreacted SCMs

3.1.1. Particle Size and Morphology (SEM)

Representative micrographs for each unreacted SCM powder obtained *via* SEM are displayed in **Figure 1**. It is known that characteristics such as particle fineness and surface area can influence both the rate and final degree of reactivity of an SCM in concrete[24]. Therefore, one of the most important physical properties of potential SCMs is the particle size[24–27]. From **Figure 1**, the powders generally appeared to range from 1-30 μm which is considered within the appropriate range for chemical reactivity[24].

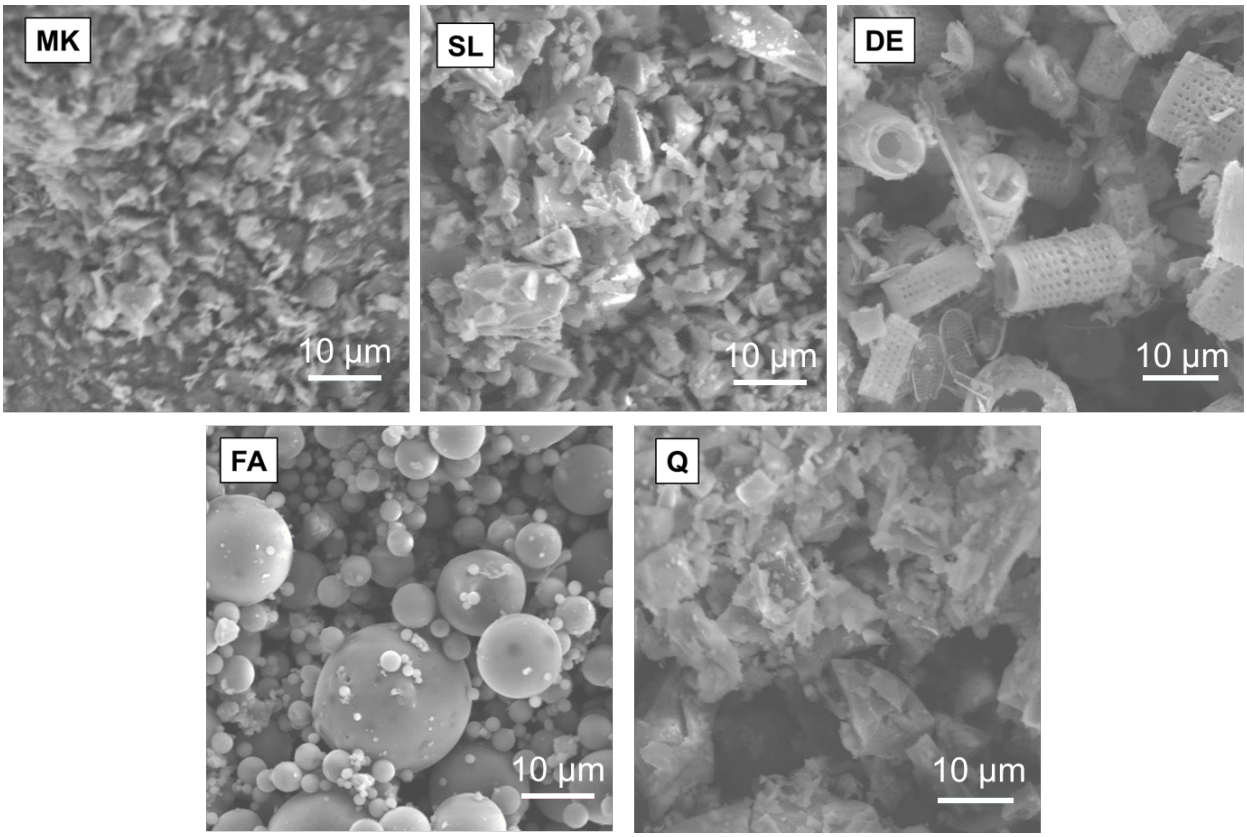

Figure 1: SEM images of unreacted SCMs. MK = metakaolin; SL = slag; DE = diatomaceous earth; FA = fly ash; Q = quartz. Scale bar = 10 µm.

Another pertinent physical property of an SCM is particle morphology, which can also be observed *via* SEM (**Figure 1**). In the currently study, MK exhibited an irregular, somewhat angular morphology. Similar characteristics have been observed in several other studies utilizing metakaolin as a cementitious material[28,29]. SL was also angular, which is attributable to the fact that ***ground*** granulated blast furnace slag requires additional crushing and grinding to a finer particle size prior to valorization as a cementitious material[30]. FA, which is known to rapidly solidify while suspended in exhaust gases, was spherical as previously reported in the literature[31]. DE particles were predominantly rod-shaped with nanostructured surface details, which has also been observed previously[32–34]. Finally, Q powder exhibited angular morphology which was expected, since the inert quartz control in this study was finely ground.

3.1.2. Chemical Composition (EDS & ICP-OES)

The elemental composition of each SCM was determined *via* EDS and substantiated using ICP-OES. The data were converted to oxide notation. The oxide compositions of each SCM are shown in **Table 3**. The data obtained *via* EDS and ICP-OES are in relatively good agreement, particularly for SiO_2, Al_2O_3, and CaO. These are the most abundant oxides and the most relevant oxides for screening cementitious materials. Notably, some variation exists because sulfur was not reported by the ICP-OES analysis, and several trace elements detected in very minor quantities by ICP-OES (*e.g.*, manganese, phosphorous) were not detected by EDS analysis. The percentage differences between the oxide compositions estimated by ICP-OES and EDS were also calculated for each SCM and provided in **Table 3**.

ASTM C618[35] can be used to classify all the materials except for SL by chemical composition. According to this standard, MK, DE, and Q each meet the chemical requirements for classification as a Class N natural pozzolan. These requirements are that the sum of SiO_2, Al_2O_3, and Fe_2O_3 must be greater than or equal to 70 wt%, and the maximum SO_3 content is 4 wt%. By ICP-OES analysis, the sums of SiO_2, Al_2O_3, and Fe_2O_3 for MK, DE, and Q are 96.91, 96.95, and 98.24 wt%, respectively. The same values for MK, DE, and Q measured by EDS are 97.54, 98.38, and 99.53 wt%, respectively. Sulfur was not detected in MK, DE, or Q; therefore, their corresponding SO_3 concentration were assumed to be zero. FA met the chemical requirements for a Class F fly ash according to ASTM C618 (the sum of SiO_2, Al_2O_3, and Fe_2O_3 must be greater than or equal to 50 wt%, and the maximum CaO and SO_3 concentrations are 18 and 5 wt%, respectively).

Table 3: Oxide compositions for the SCMs calculated from elemental compositions determined via ICP-OES (n=1) and EDS (n=5), and the % difference between the methods.

SCM/ Method		Oxide Composition (wt%)											
		SiO_2	**Al_2O_3**	**CaO**	**Fe_2O_3**	**MgO**	**K_2O**	**Na_2O**	**SO_3**	**TiO_2**	**CuO**	**MnO**	**P_2O_5**
MK	ICP	51.45	45.07	0.07	0.39	0.05	0.28	0.76	-	1.56	-	0.00	0.36
	EDS	52.78	44.76	-	-	-	-	0.18	-	2.28	-	-	-
Difference		3%	1%	N/A	N/A	N/A	N/A	125%	N/A	37%	N/A	N/A	N/A
SL	ICP	32.25	13.34	44.27	0.87	6.45	0.62	0.70	-	0.50	-	0.14	0.86
	EDS	26.01	10.87	52.02	0.79	4.66	0.38	-	4.65	0.63	-	-	-
Difference		21%	20%	16%	9%	32%	49%	N/A	N/A	23%	N/A	N/A	N/A
DE	ICP	91.62	4.35	0.66	0.98	0.58	0.31	0.62	-	0.26	-	0.01	0.62
	EDS	91.27	5.64	0.70	1.47	0.59	-	-	-	0.26	0.07	-	-
Difference		0%	26%	6%	40%	2%	N/A	N/A	N/A	0%	N/A	N/A	N/A
FA	ICP	56.05	26.20	5.27	3.87	0.99	1.94	3.53	-	0.99	-	0.03	1.14
	EDS	53.39	26.05	6.58	7.09	0.92	1.28	1.62	1.28	1.78	-	-	-
Difference		5%	1%	22%	59%	6%	41%	74%	N/A	57%	N/A	N/A	N/A
Q	ICP	97.29	0.91	0.08	0.04	0.03	0.74	0.39	-	0.04	-	0.00	0.48
	EDS	95.35	4.18	-	-	-	0.47	-	-	-	-	-	-
Difference		2%	129%	N/A	N/A	N/A	45%	N/A	N/A	N/A	N/A	N/A	N/A

The position of each SCM on a ternary SiO_2-Al_2O_3-CaO diagram is shown in **Figure 2**. As expected, reagent-grade Q was comprised of almost entirely SiO_2 with trace amounts of Al_2O_3. DE was comprised of mainly SiO_2 with trace amounts of Al_2O_3, CaO, Fe_2O_3, MgO, TiO_2, and others. DE contained ~91 wt% SiO_2. The silica concentration of diatomaceous earth used in the construction materials literature typically ranges from approximately 75 – 95 wt% SiO_2 [36–38]. MK contained just over 50 wt% SiO_2 with Al_2O_3 as the majority of the remaining fraction, with trace amounts of TiO_2. Similar oxide compositions have been reported in the literature for pure metakaolin[29,39–41].

Because they are industrial waste products, the composition of fly ash and slag varies widely in the literature. FA and SL were the only SCMs investigated herein to contain >1 wt% CaO. The CaO content of the FA was <10 wt%, which was expected since it was classified as Class F. Accordingly, FA was expected to exhibit primarily pozzolanic reactivity as opposed to hydraulic reactivity. On the other hand, SL contained ~50 wt% CaO which suggested that it would exhibit primarily latent hydraulic reactivity.

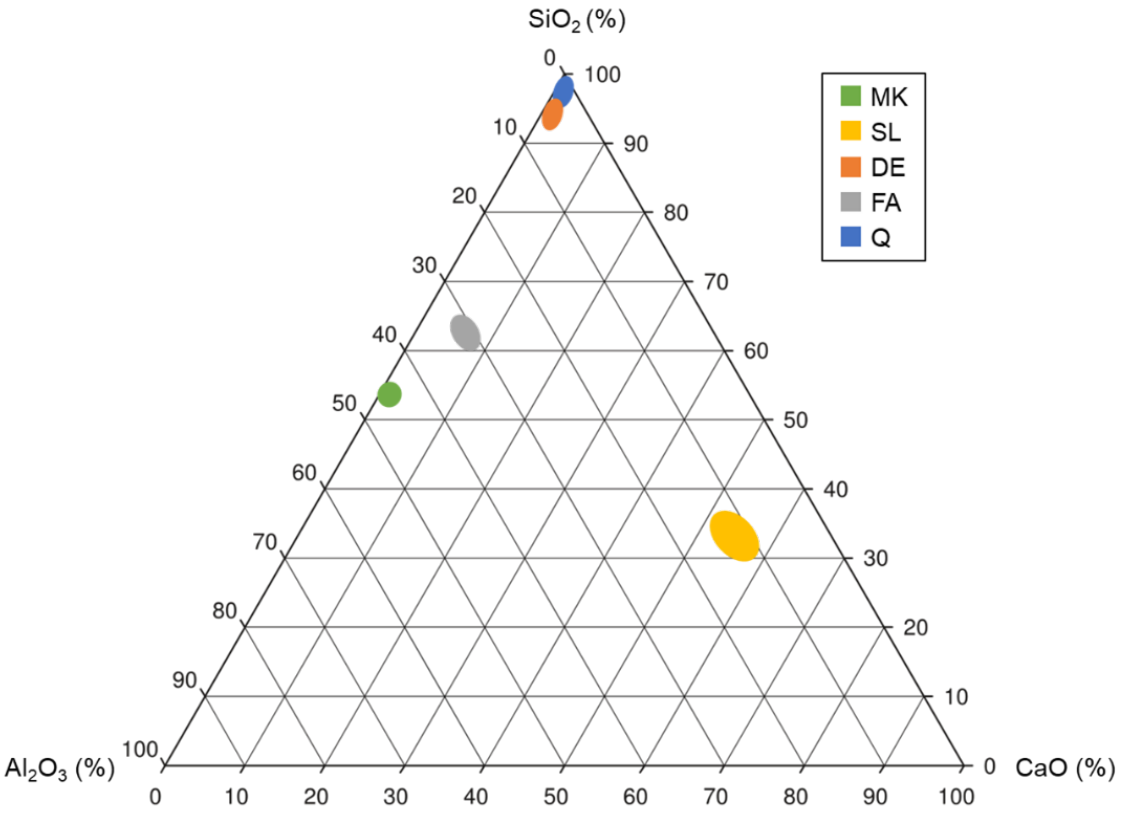

Figure 2: Ternary diagram for the primary oxide composition of unreacted SCMs.

3.1.3. Mineralogy (XRD)

Qualitative XRD was performed to investigate the mineralogy of each unreacted SCM powder, and these data are shown in **Figure 3**. As expected, Q (**Figure 3e**) was highly crystalline while the MK, SL, DE, and FA (**Figures 3a-d**) were mostly amorphous and partially crystalline. For predominantly siliceous and aluminosiliceous (*i.e.*, non-hydraulic, low calcium) materials such as MK, DE, FA, and Q, amorphous content is known to correlate well with pozzolanic reactivity[42,43]. Therefore, these data, taken together with oxide analysis data from **Table 3**, suggested that MK, DE, and FA would likely exhibit some degree of pozzolanic reactivity while Q would likely exhibit little to no reactivity.

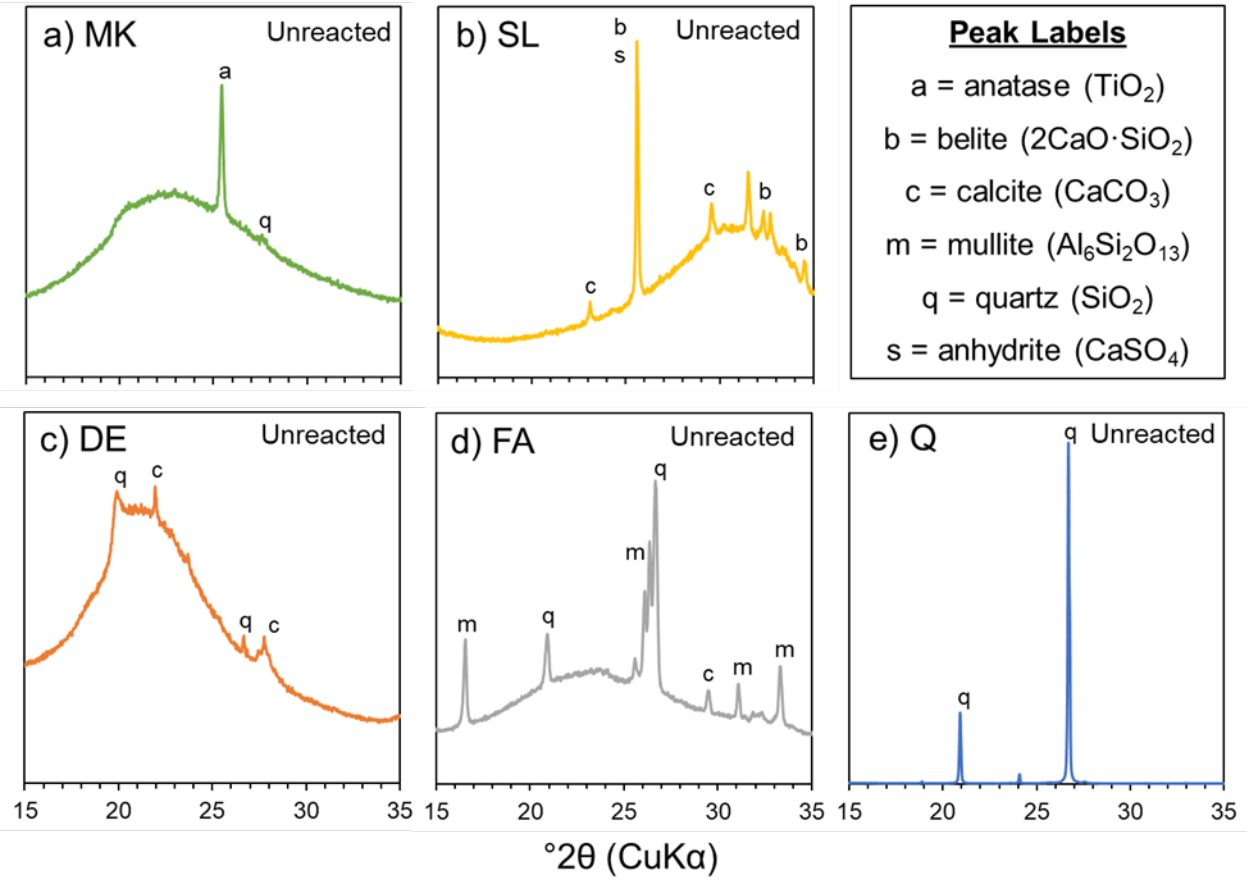

Figure 3: XRD diffractograms of unreacted a) MK = metakaolin, b) SL = slag, c) DE = diatomaceous earth, d) FA = fly ash, and e) Q = quartz.

As displayed in **Figure 3a**, MK exhibited slight peaks that matched with anatase (TiO_2). This result was expected since >1 wt.% TiO_2 was detected in the MK powder in the previous section (*see* **Table 3**), and previous studies have shown the presence of trace amounts of anatase in metakaolin *via* XRD analysis[39,44–46]. Metakaolin is formed by thermal dehydroxylation of kaolinite at temperatures typically between 600 and 800 °C depending upon the properties of the raw clay [47]. Notably, no kaolinite peaks were detected, suggesting that the aluminosilicate phases in the MK had been successfully converted to amorphous metakaolinite by thermal activation. SL was partially amorphous with slight peaks matching belite, calcite, and anhydrite. The mineralogy of blast furnace slags in the literature ranges from completely amorphous depolymerized calcium silicate glasses[48–50] to partially crystalline, often containing crystalline calcium silicates[51], calcite, quartz, and anhydrite or gypsum[52].

DE exhibited an almost entirely amorphous structure, with very slight peaks matching those of calcite and quartz (**Figure 3c**). Similar results were obtained for diatomaceous earth samples by Li *et al.*[53] and Hassan *et al.*[38]. FA was the most mineralogically complex of the materials surveyed herein, which was anticipated, given that fly ash exhibits the greatest chemical and physical variability of conventional SCMs[54]. Peaks corresponding mainly to mullite, calcite, and quartz were detected in FA (**Figure 3d**). Several studies containing XRD analyses of siliceous Class F fly ashes reported the presence of similar mineral phases, particularly mullite[55–61].

3.2. Characterization of Reacted ASTM C1897 Mixtures

3.2.1. Cumulative Heat Release (ASTM C1897 - Method A)

Heat evolution was determined according to ASTM C1897 Method A for the full-scale mixtures. Results for cumulative heat release are shown in **Figure 4**. Very low 7-day cumulative heat (23 J/g SCM) was detected for samples containing Q powder, which confirmed that it was inert, as expected. Several studies in the literature have included a similar inert quartz control and have reported 7-day cumulative heat values ranging from 21-25 J/g SCM[9,20,21], which is in agreement with the current study. As expected, the remaining SCM powders each exhibited some degree of reactivity, as indicated by heat release within 24 hours.

The highest rate of heat evolution (*i.e.*, heat flow) as well as the highest 7-day cumulative heat release was detected for MK (910 J/g SCM) followed by SL (682 J/g SCM), DE (592 J/g SCM), and FA (218 J/g SCM). Reports in the literature for 7-day cumulative heat release of ASTM C1897 samples containing calcined clay range from approximately 500 – 980 J/g SCM, depending upon the chemical purity and other properties of the calcined clay[9,21]. It was anticipated that the MK in the current study would exhibit reactivity on the higher end of similar calcined clays reported in the literature since the concentrations of SiO_2 and Al_2O_3 were considerably high (*see* **Table 3**) as was the amorphous content (*see* **Figure 3a**), indicating high purity.

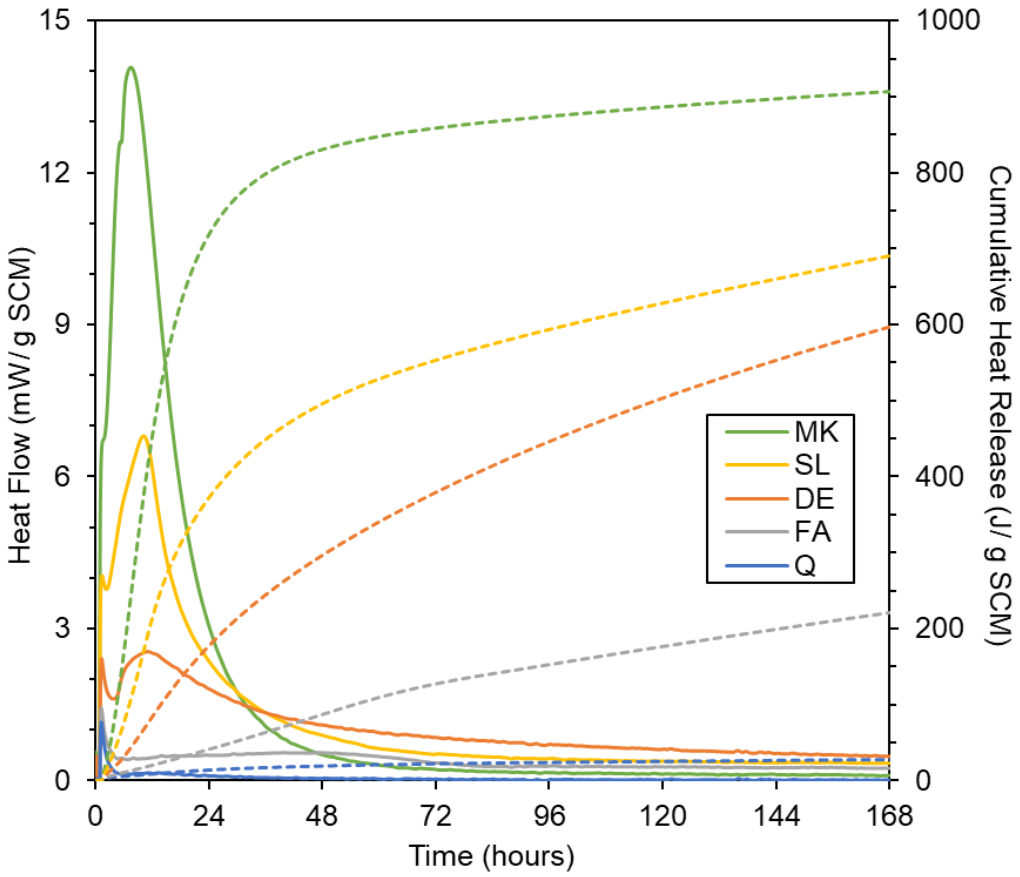

Figure 4: Representative results for pastes containing each SCM from isothermal calorimetry at 40 °C for 7 days. The rate of heat evolution and cumulative heat release are shown by solid and dashed lines, respectively.

The latent hydraulic SL exhibited the second highest 7-day cumulative heat release (682 J/g SCM) of the materials surveyed. Kancir *et al.*[62] reported that a blast furnace slag released 451 J/g SCM over 3 days, which was similar to the 3-day cumulative heat release of SL in the current study (551 J/g SCM). The natural pozzolan DE released 379 J/g SCM and 592 J/g SCM over the time periods of 3 days and 7 days, respectively. Although reasonably similar 7-day heat release measurements were obtained for SL and DE (*i.e.*, <100 J/g SCM difference, in the moderately-to-highly reactive range), the rate of reaction was substantially greater for SL than for DE. This trend is represented by the magnitude of the heat flow (solid lines) and the slope of the heat flow (dashed lines) shown in **Figure 4**.

FA exhibited a substantially lower rate of heat evolution and total evolved heat than MK, SL, and DE. However, it was indeed reactive, releasing 218 J/g SCM over 7 days as compared to

23 J/g SCM for the inert control Q. This is in agreement with Snellings *et al*.[27], where a Class F siliceous fly ash released 225 J/g SCM over 7 days, and reactivity was subsequently increased (up to 375 J/g SCM) by milling and classification treatments. The same study reported a 3-day cumulative heat release of approximately 110 J/g SCM for the plain Class F fly ash, yielding a 3-day to 7-day cumulative heat release ratio of 0.49[27]. The 3-day cumulative heat release and the 3-day to 7-day cumulative heat release ratio for FA in the current study were 126 J/g SCM and 0.58, respectively.

3.2.2. Bound Water Measurements (ASTM C1897 - Method B)

Chemically bound water was determined according to ASTM C1897 Method B for the full-scale mixtures using a furnace. The data for bound water measurements are displayed in **Figure 5**. Very good correlation ($R^2 = 0.9662$) was obtained between the bound water content and cumulative heat release, which is also shown in **Figure 5**. The samples containing inert Q contained 1.04 ± 0.09 g of bound water per 100 g dried paste. Other studies that have included inert quartz control samples have reported bound water contents ranging from 0.3 – 2.15 g/100 g dried paste[9,20,21,56,63]. Samples containing the highly reactive MK powder contained 16.71 ± 0.17 g of bound water per 100 g dried paste. ASTM C1897 bound water content for calcined clays has been previously reported in the literature to range from 7.5 – 14.0 g/100 g dried paste[9,21,56].

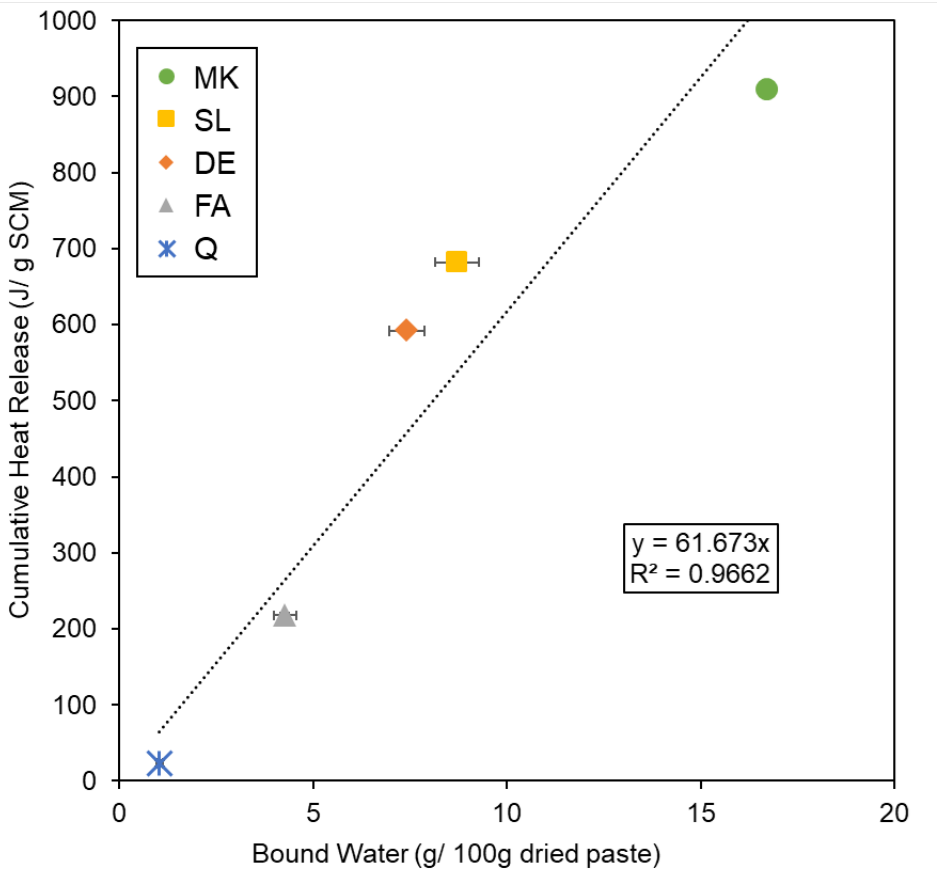

Figure 5: Chemically bound water (Method B) vs. cumulative heat release (Method A) for full-scale ASTM C1897 samples. Bound water content was measured by calculating the mass loss between 40°C and 350°C. Horizontal error bars represent the range for duplicate samples; vertical error bars represent the standard deviation for triplicate samples. In most instances, the error bars are small and, thus, obfuscated by the data point marker.

Samples containing SL and DE contained 8.71 ± 0.57 and 7.43 ± 0.46 g of bound water per 100 g dried paste, respectively. ASTM C1897 bound water data for blast furnace slags in the literature ranges from 4.9 – 8.5 g/ g dried paste[20,21,27]; no previously published bound water data was found for diatomaceous earth. FA contained 4.27 ± 0.29 g of bound water per 100 g dried paste in the current study. Fly ashes in the literature have exhibited bound water contents ranging from 1.9 – 7.5 g/ g dried paste, and generally calcareous type C fly ashes had higher bound water contents than siliceous type F fly ashes[9,20,21,64].

3.2.3. Thermogravimetric Analysis

Results for bound water content determined *via* TGA for full-scale, mid-scale, and small-scale mixtures containing each SCM are displayed in **Figure 6,** alongside the bound water content measured on full-scale samples using the furnace method in the previous section. Bound water content measurements for the full-scale samples were extremely consistent ($R^2 = 0.99$) regardless of measurement technique (*i.e.*, furnace, TGA). This result is supported by Wang *et al.*[65] in which high correlation ($R^2 = 0.96$) was observed between full-scale R3 bound water measurements obtained using a furnace and TGA. It is also evident from **Figure 6** in the current study that bound water was consistent regardless of scale. In fact, the bound water contents determined for each SCM determined via TGA at each mass scale (*i.e.*, full, mid, small) were ranked in the same order as for the full-scale furnace bound water content where MK > SL > DE > FA > Q.

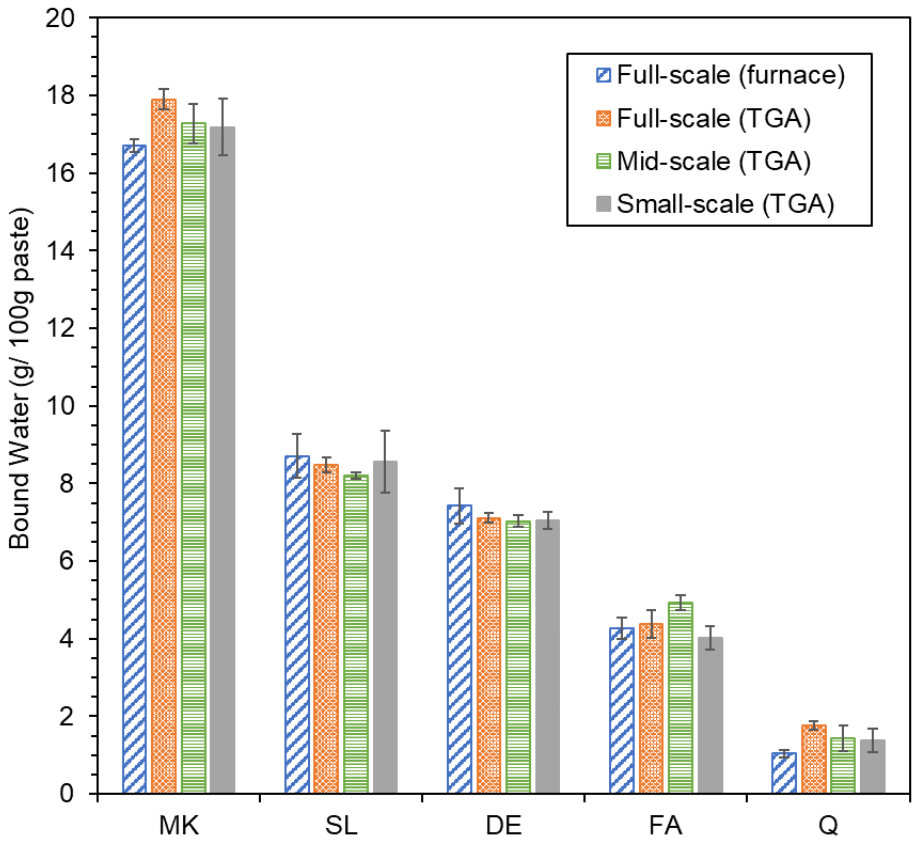

Figure 6: Bound water content at all scales. Bound water content was measured by calculating the mass loss between 40°C and 350°C. Error bars represent the standard deviation for triplicate samples.

3.2.4. Statistical Analysis (Mann-Whitney U Tests)

A summary of statistical two-tailed Mann-Whitney U Tests, shown in **Table 4**, were performed to confirm that the data were statistically similar across all scales and measurement techniques. Scenario 1 demonstrated that, for the full-scale ASTM C1897 samples, bound water content measured *via* TGA was statistically similar (*i.e.*, $U>U_{critical}$) to bound water content measured using a furnace. Scenarios 2 and 3 compared the full-scale furnace data to mid-scale and small-scale TGA data, respectively, and the outcome of both scenarios was statistical similarity. Finally, scenario 4 showed that the full-scale and small-scale TGA data were statistically similar.

Table 4: Summary of two-tailed Mann-Whitney U tests performed on bound water data. For each scenario: $\alpha = 0.05$, $n_1 = n_2 = 15$, and $U_{critical} = 64$.

	Group 1		**Group 2**			
Scenario	*Scale*	*Method*	*Scale*	*Method*	U	**Are Groups 1 and 2 statistically different (*i.e.*, $U_{critical}>U$)?**
1	Full	Furnace	Full	TGA	107	No
2	Full	Furnace	10^{-2}	TGA	106	No
3	Full	Furnace	10^{-3}	TGA	111	No
4	Full	TGA	10^{-3}	TGA	93	No

3.2.5. Mineralogy (XRD)

Qualitative XRD was performed on each paste mixture at both the full-scale and small-scale to interrogate the influence of scale on mineralogy. These data are shown in **Figure 7**. From **Figure 7**, it is evident that the sample scale did not influence mineralogy of the reacted paste mixtures. Crystalline portlandite was detected in all samples; this was expected since the SCM-to-portlandite ratio of 1:3 in the R3 test is designed to provide excess portlandite to ensure a complete pozzolanic reaction. Additionally, reaction products including calcium silicate hydrate and ettringite were detected in mixtures containing the reactive MK, SL, DE, and FA. Due to the overlapping nature of the peaks for calcite (which is added to the R3 pastes as an excess counter anion for the alumina-bearing phases[22,64]) and poorly crystalline CSH at ~29° 2θ, it was not attempted to interpret the presence and/or relative intensities of CSH phases.

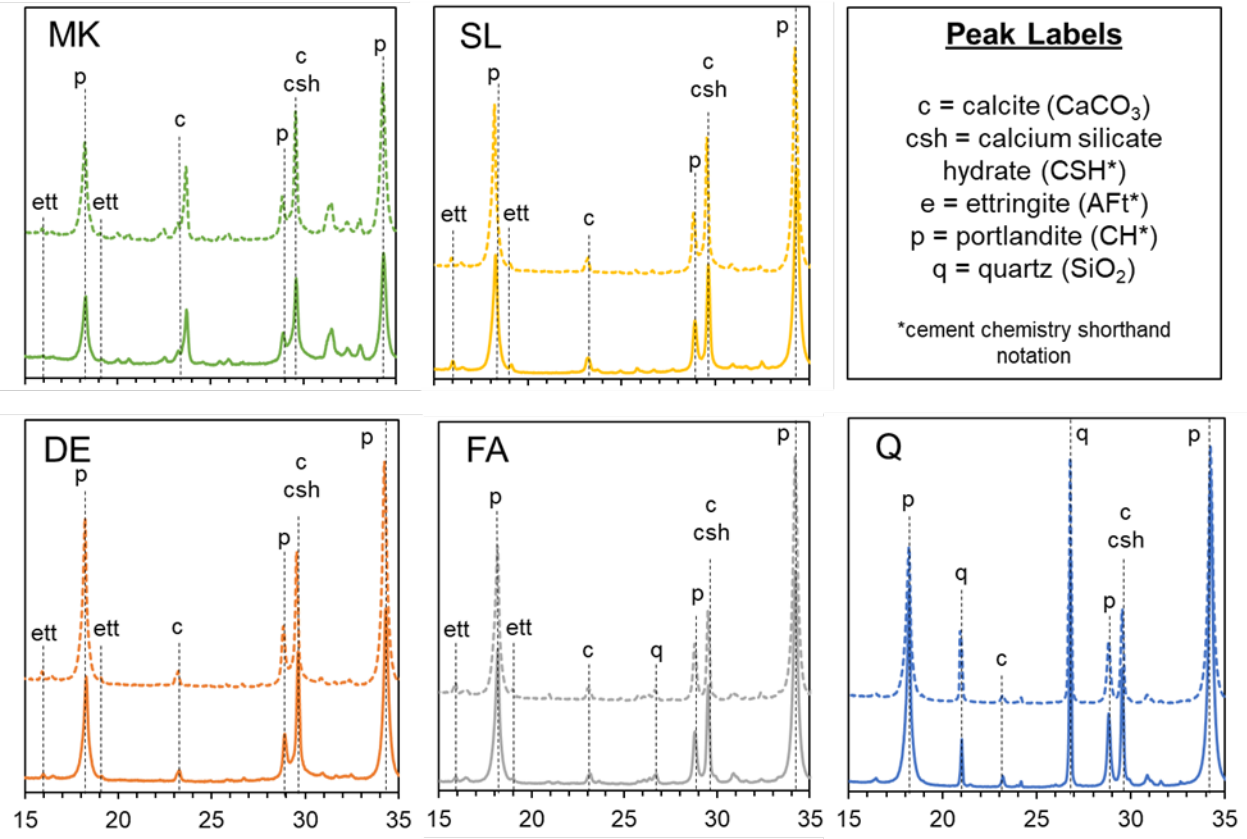

Figure 7: XRD diffractograms of full-scale (solid lines) and small-scale (dashed lines) reacted R3 pastes.

3.3 Significance and Limitations

In this study, it was substantiated that the R3 bound water content test could be performed with sufficient accuracy at a significantly smaller sample size than has been shown previously in the literature. Five different SCMs spanning a wide range of reactivities were tested according to both the ASTM C1897 isothermal calorimetry (method A) and bound water (method B) procedures at the full-scale (*i.e.*, 15 g). The results were in good agreement with the literature, and good correlation (R^2 = 0.9662) was obtained between the two methods. Bound water content was also evaluated for each of the five SCMs at the full, mid, and small-scale (*i.e.*, 10^0, 10^{-2}, 10^{-3} scale) *via* TGA. The bound water contents appeared reasonably consistent for each SCM regardless of the measurement technique (*i.e.*, furnace vs TGA) or the mass scale (*i.e.*, full, mid, small). Statistical similarity was confirmed by a series of statistical Mann-Whitney U Tests.

The results from this methodological study could be interpreted as a modified R3 test that significantly reduces the sample size requirement from approximately 2 g of SCM per test to as low as 10 mg per test. This milligram-scale thermogravimetric method enables very high-throughput reactivity screening of alternative SCMs. Using this method, researchers can now screen multiple alternative SCM sources and treatments thereof using milligram-scale quantities. Combined with machine learning and artificial intelligence, optimal physical and chemical treatment methods to improve alternative SCM reactivity could be elucidated using this method. Researchers should take caution in applying this approach to quarried and/or waste minerals that are substantially more heterogeneous than the minerals investigated herein. For more chemically heterogeneous materials, sampling requirements such as those stipulated in ASTM C311 may need to be followed to ensure that representative samples of each SCM are obtained and tested. Additionally, whether it is conducted at the full-scale described in the ASTM C1897 standard or the small-scale described herein, the R3 test should be considered an initial screening method to determine chemical reactivity. Further experimental testing including trial batching and durability testing is required prior to implementation in real world concrete mixtures.

It is anticipated that the small-scale R3 bound water method developed herein will enable high-throughput screening of more diverse materials that might currently be available only in small quantities, such as manufactured, biomanufactured, and/or synthetic materials that do not yet have a consistent supply chain. Such a method could facilitate and accelerate the discovery of new SCMs that will alleviate the challenges associated with increasing demand and diminishing global supply of SCMs that are currently used around the world.

4. CONCLUSIONS

In the current study, a small-scale thermogravimetric method to measure the chemical reactivity of minerals based on the principles of the R3 test was designed and validated. The results from this methodological study could be interpreted as a modified R3 test that significantly reduces sample size requirements, which could in turn enable rapid, high-throughput screening of novel SCMs that are needed to accelerate the decarbonization of the global cement and concrete industry.

1. ASTM C1897 cumulative heat (Method A) and bound water (Method B) were determined for metakaolin, a slag, diatomaceous earth, a fly ash, and inert quartz using the standard sample size of 15 g of hydrated paste (*i.e.*, full-scale). Excellent

correlation ($R^2 = 0.9662$) was obtained between the two methods, and the results were also in good agreement with the literature.

2. Paste samples were prepared across different orders of magnitude by mass (*i.e.*, full-scale (10^0), mid-scale (10^{-2}), and small-scale (10^{-3})) for bound water testing using TGA. By inspection, the results appeared to be consistent regardless of sample size or measurement technique.
3. A two-tailed Mann-Whitney U test indicated no statistical difference between the bound water measurements obtained by the full-scale method and the small-scale thermogravimetric method proposed herein.

5. Acknowledgements:

This research was made possible by the Department of Civil, Environmental, and Architectural Engineering, the Materials Science and Engineering Program, the College of Engineering and Applied Sciences, and the Living Materials Lab at the University of Colorado, Boulder. This research was supported, in part, by the Colorado Shared Instrumentation in Nanofabrication and Characterization (COSINC): the COSINC-CHR (Characterization), College of Engineering & Applied Science, University of Colorado Boulder. The authors would like to acknowledge the support of the staff (Tomoko Borsa) and the facility that have made this work possible (scanning electron microscopy and electron dispersive spectroscopy analysis). The authors would also like to acknowledge the help of scientists at Hazen Research (inductively coupled plasma analysis). This material is based upon work supported by the National Science Foundation under Grant No. CMMI-1943554. Any opinions, findings, and conclusions or recommendations expressed in this material are those of the authors and do not necessarily reflect the views of the National Science Foundation.

6. REFERENCES

1. US Geological Survey. *Mineral Commodity Summaries*. (2021).
2. Lehne, J. & Preston, F. *Making Concrete Change: Innovation in Low-carbon Cement and Concrete*. (2018).

3. Juenger, M. C. G., Snellings, R. & Bernal, S. A. Supplementary cementitious materials: New sources, characterization, and performance insights. *Cement and Concrete Research* **122**, 257–273 (2019).
4. Scrivener, K. L., John, V. M. & Gartner, E. M. Eco-efficient cements: Potential economically viable solutions for a low-CO2 cement-based materials industry. *Cement and Concrete Research* **114**, 2–26 (2018).
5. Dhandapani, Y. & Santhanam, M. Investigation on the microstructure-related characteristics to elucidate performance of composite cement with limestone-calcined clay combination. *Cement and Concrete Research* **129**, 105959 (2020).
6. McCarthy, M. J., Robl, T. & Csetenyi, L. J. Recovery, processing, and usage of wet-stored fly ash. in *Coal Combustion Products (CCP's)* 343–367 (Elsevier, 2017). doi:10.1016/B978-0-08-100945-1.00014-9.
7. Adriano, D. C., Page, A. L., Elseewi, A. A., Chang, A. C. & Straughan, I. Utilization and Disposal of Fly Ash and Other Coal Residues in Terrestrial Ecosystems: A Review. *J. environ. qual.* **9**, 333–344 (1980).
8. Finkelman, R. B., Wolfe, A. & Hendryx, M. S. The future environmental and health impacts of coal. *Energy Geoscience* **2**, 99–112 (2021).
9. Li, X. *et al.* Reactivity tests for supplementary cementitious materials: RILEM TC 267-TRM phase 1. *Mater Struct* **51**, 151 (2018).
10. ASTM International. *Test Methods for Sampling and Testing Fly Ash or Natural Pozzolans for Use in Portland-Cement Concrete*. http://www.astm.org/cgi-bin/resolver.cgi?C311C311M-18 (2018) doi:10.1520/C0311_C0311M-18.

11. Kalina, R. D., Al-Shmaisani, S., Ferron, R. D. & Juenger, M. C. G. False Positives in ASTM C618 Specifications for Natural Pozzolans. *ACI Materials Journal* **116**, (2019).
12. Wang, Y., Burris, L., Shearer, C. R., Hooton, D. & Suraneni, P. Strength activity index and bulk resistivity index modifications that differentiate inert and reactive materials. *Cement and Concrete Composites* **124**, 104240 (2021).
13. Donatello, S., Tyrer, M. & Cheeseman, C. R. Comparison of test methods to assess pozzolanic activity. *Cement and Concrete Composites* **32**, 121–127 (2010).
14. Tantawy, M. A. Characterization and pozzolanic properties of calcined alum sludge. *Materials Research Bulletin* **61**, 415–421 (2015).
15. Chapelle, J. Attaque sulfocalcique des laitiers et pouzzolanes. *Revue des Matériaux de Construction* **512**, 136–145 (1958).
16. Avet, F., Snellings, R., Alujas Diaz, A., Ben Haha, M. & Scrivener, K. Development of a new rapid, relevant and reliable (R3) test method to evaluate the pozzolanic reactivity of calcined kaolinitic clays. *Cement and Concrete Research* **85**, 1–11 (2016).
17. Suraneni, P., Hajibabaee, A., Ramanathan, S., Wang, Y. & Weiss, J. New insights from reactivity testing of supplementary cementitious materials. *Cement and Concrete Composites* **103**, 331–338 (2019).
18. Suraneni, P. Recent developments in reactivity testing of supplementary cementitious materials. *RILEM Tech Lett* **6**, 131–139 (2021).
19. Choudhary, A., Bharadwaj, K., Ghantous, R. M., Isgor, O. B. & Weiss, J. Pozzolanic Reactivity Test of Supplementary Cementitious Materials. *MJ* **119**, (2022).
20. Sivakumar, P. P., Matthys, S., De Belie, N. & Gruyaert, E. Reactivity Assessment of Modified Ferro Silicate Slag by R3 Method. *Applied Sciences* **11**, 366 (2021).

21. Gholizadeh Vayghan, A. *et al.* Use of Treated Non-Ferrous Metallurgical Slags as Supplementary Cementitious Materials in Cementitious Mixtures. *Applied Sciences* **11**, 4028 (2021).
22. ASTM International. *Standard Test Methods for Measuring the Reactivity of Supplementary Cementitious Materials by Isothermal Calorimetry and Bound Water Measurements*. http://www.astm.org/cgi-bin/resolver.cgi?C1897-20 (2020) doi:10.1520/C1897-20.
23. Ho, A. D. A Nonparametric Framework for Comparing Trends and Gaps Across Tests. *Journal of Educational and Behavioral Statistics* **34**, 201–228 (2009).
24. Mirzahosseini, M. & Riding, K. A. Influence of different particle sizes on reactivity of finely ground glass as supplementary cementitious material (SCM). *Cement and Concrete Composites* **56**, 95–105 (2015).
25. Juenger, M. C. G. & Siddique, R. Recent advances in understanding the role of supplementary cementitious materials in concrete. *Cement and Concrete Research* **78**, 71–80 (2015).
26. Glosser, D., Choudhary, A., Isgor, O. B. & Weiss, W. J. Investigation of the Reactivity of Fly Ash and Its Effect on Mixture Properties. *ACI Materials Journal* **116**, (2019).
27. Snellings, R., Kazemi-Kamyab, H., Nielsen, P. & Van den Abeele, L. Classification and Milling Increase Fly Ash Pozzolanic Reactivity. *Front. Built Environ.* **7**, 670996 (2021).
28. Zhang, S., Zhou, Y., Sun, J. & Han, F. Effect of Ultrafine Metakaolin on the Properties of Mortar and Concrete. *Crystals* **11**, 665 (2021).
29. Mierzwiński, D. *et al.* Thermal phenomena of alkali-activated metakaolin studied with a negative temperature coefficient system. *J Therm Anal Calorim* **138**, 4167–4175 (2019).
30. Wan, H., Shui, Z. & Lin, Z. Analysis of geometric characteristics of GGBS particles and their influences on cement properties. *Cement and Concrete Research* **34**, 133–137 (2004).

31. Yang, T. *et al.* Effect of fly ash microsphere on the rheology and microstructure of alkali-activated fly ash/slag pastes. *Cement and Concrete Research* **109**, 198–207 (2018).
32. Sedai, B. R. *et al.* Particle morphology dependent superhydrophobicity in treated diatomaceous earth/polystyrene coatings. *Applied Surface Science* **416**, 947–956 (2017).
33. Dobrosielska, M. *et al.* A New Method of Diatomaceous Earth Fractionation—A Bio-Raw Material Source for Epoxy-Based Composites. *Materials* **14**, 1663 (2021).
34. Jia, Y., Han, W., Xiong, G. & Yang, W. Diatomite as high performance and environmental friendly catalysts for phenol hydroxylation with H_2O_2. *Science and Technology of Advanced Materials* **8**, 106–109 (2007).
35. ASTM International. *Standard Specification for Coal Fly Ash and Raw or Calcined Natural Pozzolan for Use in Concrete*. http://www.astm.org/cgi-bin/resolver.cgi?C618-19 (2019) doi:10.1520/C0618-19.
36. Yılmaz, B. & Ediz, N. The use of raw and calcined diatomite in cement production. *Cement and Concrete Composites* **30**, 202–211 (2008).
37. Li, J., Zhang, W., Li, C. & Monteiro, P. J. M. Green concrete containing diatomaceous earth and limestone: Workability, mechanical properties, and life-cycle assessment. *Journal of Cleaner Production* **223**, 662–679 (2019).
38. Hassan, H. S. *et al.* Cleaner production of one-part white geopolymer cement using pre-treated wood biomass ash and diatomite. *Journal of Cleaner Production* **209**, 1420–1428 (2019).
39. Lee, S., Kim, B., Seo, J. & Cho, S. Beneficial Use of MIBC in Metakaolin-Based Geopolymers to Improve Flowability and Compressive Strength. *Materials* **13**, 3663 (2020).
40. Justice, J. M. & Kurtis, K. E. Influence of Metakaolin Surface Area on Properties of Cement-Based Materials. *J. Mater. Civ. Eng.* **19**, 762–771 (2007).

41. Perez-Cortes, P. & Escalante-Garcia, J. I. Design and optimization of alkaline binders of limestone-metakaolin – A comparison of strength, microstructure and sustainability with portland cement and geopolymers. *Journal of Cleaner Production* **273**, 123118 (2020).
42. Walker, R. & Pavía, S. Physical properties and reactivity of pozzolans, and their influence on the properties of lime–pozzolan pastes. *Mater Struct* **44**, 1139–1150 (2011).
43. Villar-Cociña, E., Morales, E. V., Santos, S. F., Savastano, H. & Frías, M. Pozzolanic behavior of bamboo leaf ash: Characterization and determination of the kinetic parameters. *Cement and Concrete Composites* **33**, 68–73 (2011).
44. Walkley, B., Ke, X., Hussein, O. H., Bernal, S. A. & Provis, J. L. Incorporation of strontium and calcium in geopolymer gels. *Journal of Hazardous Materials* **382**, 121015 (2020).
45. Zhang, B., MacKenzie, K. J. D. & Brown, I. W. M. Crystalline phase formation in metakaolinite geopolymers activated with NaOH and sodium silicate. *J Mater Sci* **44**, 4668–4676 (2009).
46. Weise, K., Ukrainczyk, N. & Koenders, E. A Mass Balance Approach for Thermogravimetric Analysis in Pozzolanic Reactivity R3 Test and Effect of Drying Methods. *Materials* **14**, 5859 (2021).
47. Król, M. & Rożek, P. The effect of calcination temperature on metakaolin structure for the synthesis of zeolites. *Clay miner.* **53**, 657–663 (2018).
48. Wu, Y.-H., Huang, R., Tsai, C.-J. & Lin, W.-T. Recycling of Sustainable Co-Firing Fly Ashes as an Alkali Activator for GGBS in Blended Cements. *Materials* **8**, 784–798 (2015).
49. Türker, H. T., Balçikanli, M., Durmuş, İ. H., Özbay, E. & Erdemir, M. Microstructural alteration of alkali activated slag mortars depend on exposed high temperature level. *Construction and Building Materials* **104**, 169–180 (2016).

50. Ozturk, Z. & Gultekin, E. Preparation of ceramic wall tiling derived from blast furnace slag. *Ceramics International* **41**, 12020–12026 (2015).

51. Wang, Y. & Suraneni, P. Experimental methods to determine the feasibility of steel slags as supplementary cementitious materials. *Construction and Building Materials* **204**, 458–467 (2019).

52. Park, H., Jeong, Y., Jeong, J.-H. & Oh, J. Strength Development and Hydration Behavior of Self-Activation of Commercial Ground Granulated Blast-Furnace Slag Mixed with Purified Water. *Materials* **9**, 185 (2016).

53. Li, S., Li, D., Su, F., Ren, Y. & Qin, G. Uniform surface modification of diatomaceous earth with amorphous manganese oxide and its adsorption characteristics for lead ions. *Applied Surface Science* **317**, 724–729 (2014).

54. Medepalli, S., Sharma, M. & Bishnoi, S. Blending of Fly Ashes to Reduce Variability in the Heat of Hydration and Compressive Strength. *J. Mater. Civ. Eng.* **32**, 04020046 (2020).

55. Diaz-Loya, I., Juenger, M., Seraj, S. & Minkara, R. Extending supplementary cementitious material resources: Reclaimed and remediated fly ash and natural pozzolans. *Cement and Concrete Composites* **101**, 44–51 (2019).

56. Flegar, M., Serdar, M., Londono-Zuluaga, D. & Scrivener, K. Regional Waste Streams as Potential Raw Materials for Immediate Implementation in Cement Production. *Materials* **13**, 5456 (2020).

57. Avet, F. *et al.* Report of RILEM TC 267-TRM phase 2: optimization and testing of the robustness of the R3 reactivity tests for supplementary cementitious materials. *Mater Struct* **55**, 92 (2022).

58. Du Plessis, P., Ojumu, T. & Petrik, L. Waste Minimization Protocols for the Process of Synthesizing Zeolites from South African Coal Fly Ash. *Materials* **6**, 1688–1703 (2013).
59. Yaping, Y., Xiaoqiang, Z., Weilan, Q. & Mingwen, W. Synthesis of pure zeolites from supersaturated silicon and aluminum alkali extracts from fused coal fly ash. *Fuel* **87**, 1880–1886 (2008).
60. Hower, J. C. *et al.* Generation and nature of coal fly ash and bottom ash. in *Coal Combustion Products (CCP's)* 21–65 (Elsevier, 2017). doi:10.1016/B978-0-08-100945-1.00002-2.
61. Król, M., Rożek, P. & Mozgawa, W. Synthesis of the Sodalite by Geopolymerization Process Using Coal Fly Ash. *Pol. J. Environ. Stud.* **26**, 2611–2617 (2017).
62. Kancir, I. & Serdar, M. Contribution to Understanding of Synergy between Red Mud and Common Supplementary Cementitious Materials. *Materials* **15**, 1968 (2022).
63. Muy, Y. Sédiment activé par calcination flash comme ajout minéral en substitution du ciment portland. *Academic Journal of Civil Engineering* 218-226 Pages (2021) doi:10.26168/AJCE.39.1.41.
64. Al-Shmaisani, S. *et al. Supplementary Cementitious Materials: Assessment of Test Methods for New and Blended Materials*. (2020).
65. Wang, Y. *et al.* A rapid furnace-based gravimetry test for assessing reactivity of supplementary cementitious materials. *Mater Struct* **55**, 193 (2022).